arXiv:1303.7214v1 [nucl-th] 28 Mar 2013

Glasma Evolution and Bose Condensation with Elastic and Inelastic Collisions

Xu-Guang Huang(1), Jinfeng Liao(1,2)

March 29, 2013

1. Physics Department and Center for Exploration of Energy and Matter, Indiana University, 2401 N Milo B. Sampson Lane, Bloomington, IN 47408, USA.

2. RIKEN BNL Research Center, Bldg. 510A, Brookhaven National Laboratory, Upton, NY 11973, USA.

Abstract

In this paper we investigate the role of inelastic collision in the kinetic evolution of a highly overpopulated system starting from Glasma-type initial condition. Using the Gunion-Bertsch formula we derive the inelastic collision kernel under the collinear and small angle approximations. With both numerics and analytic analysis, we show that the inelastic process has two effects: globally changing (mostly reducing) the total particle number, while locally at small p always filling up the infrared regime extremely quickly. This latter effect is found to significantly speed up the emergence of local thermal form with vanishing local "chemical potential" and catalyzes the onset of gluon condensation to occur faster (as compared with the purely elastic case) in the overpopulated Glasma.

1 Introduction

Thermalization of the quark-gluon plasma is one of the most challenging problems in current heavy ion physics. Starting with two colliding nuclei in a form of color glass condensate with high gluon occupation $f \sim 1/\alpha_{\mathrm{s}}$ below saturation scale Q_{s} [1, 2, 3] and following the initial impact, a subsequent strong field evolution stage (likely with instabilities [4]) till about the time $1/Q_{\mathrm{s}}$ is then succeeded by a far-from-equilibrium gluon-dominant matter, the Glasma [5]. The evolution this Glasma stage toward a locally equilibrated quark-gluon plasma (QGP) is strongly indicated by phenomenology to be reached on the order of a fermi over c time (see e.g. [6]). Precisely how this occurs remains to be fully understood. Describing the pre-equilibrium evolution with kinetic equations is a very useful approach, based on which the so-called "bottom-up" therma lization scenario was developed [7, 8, 9]. There is however the complication of instability driven by anisotropy that may change this picture (see e.g. [10, 11, 12, 13]). There are also other kinetic-based approaches, see e.g. [14].

More recently an alternative thermalization scenario, based on crucial role of high initial overpopulation in the Glasma and kinetic evolution dominated by elastic collisions, has been proposed in [15, 16]. In this scenario, while the initial scale Q_s is large compared with Λ_{QCD} and thus the coupling α_s is small, the high occupation $f \sim 1/\alpha_s$ elevates the elastic scattering rate to be of the order $\hat{O}(1)$ rather than the usual $\hat{O}(\alpha_s^2)$, and the Glasma is essentially an emergent strongly interacting matter with weak coupling albeit large aggregate of constituents. Two important scales are introduced to characterize the distribution, the hard cut-off scale Λ beyond which $f << 0$ and the soft high-occupation scale Λ_s below which $f \sim 1/\alpha_s$. While the initial Glasma has the two scales overlapping $\Lambda \sim \Lambda_s \sim Q_s$, during the course of thermalization the two scales are separated eventually toward $\Lambda_s \sim \alpha_s \Lambda$ upon thermalization. One particularly nontrivial observation in the elastic-dominant picture is that the high initial overpopulation $n/\epsilon^{3/4} \sim 1/a_s^{1/4} >> 1$ and the conservation of both energy and particle number will necessarily require the formation of a Bose-Einstein condensate that absorbs the excess gluons. This has been explicitly shown to occur by numerically solving the elastic kinetic equation derived under small angle approximation [16]. There have been intensive discussions related to this picture from a variety of approaches, see e.g. [17, 18, 19, 20, 21, 22, 23, 24, 25, 26, 27, 28, 29, 30, 31, 32]. Strong evidences for the formation of such a Bose condensate have been reported for similar thermalization problem in the classical-statistical lattice simulation of scalar field theory [19, 20, 21]. The case for non-Abelian gauge theory is more complicated and still under investigation [22, 23, 24, 25, 26].

One important question that has not been addressed in the above scenario is the role of inelastic processes. This issue could indeed be critical for at least two reasons (see discussions in e.g. [15, 16, 17, 18, 31, 32]). First of all the inelastic processes will spoil the particle number conservation, and one might naively argue that the excessive gluons in the overpopulated Glasma could simply be eliminated by very fast inelastic collisions. Secondly, to make it even worse, the inelastic processes are parametrically at the same order as the elastic processes (as opposed to naive power counting), so there appears no apparent dominance of the elastic over the inelastic and one may indeed worry that the inelastic could efficiently reduce total particle number. In such a situation, an explicit evaluation including both elastic and inelastic collisions becomes mandatory to clarify what will happen after including both t ypes of collisions. To be precise, once the inelastic processes are included, one does not expect any condensation in the ultimate thermal equilibrium because with long enough time the inelastic processes will always remove any excessive particles. The real question is, while in the purely elastic case the overpopulated system is driven toward a dynamical onset of condensation in a finite time, whether the inelastic processes will even remove this transient off-equilibrium condensation or what else could happen.

In this paper, we aim to address this important question by studying the kinetic evolution of a highly overpopulated system starting from Glasma-type initial condition with both $2 \leftrightarrow 2$ and $2 \leftrightarrow 3$ scatterings. In Section 2 we will derive the inelastic collision kernel under the collinear and small angle approximations using the Gunion-Bertsch formula. In Section 3 we will use numerical solutions as well as analytic analysis to understand the role of the inelastic process for both the global particle number change and the local behavior at small momentum region. Finally we will conclude in Section 4. As a first step toward understanding the inelastic contributions and for simplicity and unambiguity, we will focus on the static box case with isotropic distribution in this work and leave the study of expanding case for future work.

2 Kinetic Evolution with Elastic and Inelastic Collisions

In this section we will derive the kinetic evolution equation with both elastic and inelastic collisions. The kinetic equation deals with the gluon distribution function defined as:

$$f(t, \mathbf{x}, \mathbf{p}) \equiv \frac{(2\pi)^3}{N_g} \frac{dN}{d^3\mathbf{x} d^3\mathbf{p}}. \tag{1}$$

The $N_g = 2(N_c^2 - 1)$ denotes the spin and color degeneracy factor. The Boltzmann equation for $f(t, \mathbf{x}, \mathbf{p})$ reads

$$\mathcal{D}_t f_p = \mathcal{C}_{2\leftrightarrow 2}[f_p] + \mathcal{C}_{2\leftrightarrow 3}[f_p], \tag{2}$$

where we denote $f(t, \mathbf{x}, \mathbf{p})$ by f_p and

$$\mathcal{D}_t \equiv \frac{p^\mu}{E_p} \partial_\mu = \partial_t + \mathbf{v}_p \cdot \nabla_{\mathbf{x}} \tag{3}$$

with $\mathbf{v}_p \equiv \mathbf{p}/E_p$ and $E_p = |\mathbf{p}|$. For later convenience, we also introduce the following notations:

$$g_p \equiv 1 + f_p \ , \ h_p \equiv f_p \, g_p = f_p(1 + f_p) \ . \tag{4}$$

In what follows we will separately discuss the elastic term $\mathcal{C}_{2\leftrightarrow 2}$ and the inelastic term $\mathcal{C}_{2\leftrightarrow 3}$.

2.1 The $2 \leftrightarrow 2$ process

The collision kernel from the $2 \leftrightarrow 2$ process with full nonlinearity has been studied in [15, 16]. Here we only briefly summarize the main results. We have the $2 \rightarrow 2$ collision matrix element square to be:

$$|M_{2\leftrightarrow 2}|^2 = 8g^4 N_c^2 N_g \left(3 - \frac{tu}{s^2} - \frac{su}{t^2} - \frac{ts}{u^2}\right). \tag{5}$$

The $2 \leftrightarrow 2$ collision kernel is then

$$\begin{aligned} \mathcal{C}_{2\leftrightarrow 2}[f_p] &= \frac{1}{N_g}\frac{1}{2}\int_{123} \frac{1}{2E_p} |M_{12\rightarrow 3p}|^2 (2\pi)^4 \delta^4(p_1 + p_2 - p_3 - p) \\ &\quad \times [(1+f_p)(1+f_3)f_1 f_2 - f_p f_3 (1+f_1)(1+f_2)], \end{aligned} \tag{6}$$

where

$$\int_i \equiv \int \frac{d^3\mathbf{p}_i}{(2\pi)^3 2E_i}. \tag{7}$$

The pre-factor $1/2$ is a symmetry factor counterweighing the permutation of 1 and 2 while the pre-factor $1/N_g$ cancels the summation over the spin and color of gluon "p" in the matrix element square (5).

The dominant contribution of $2 \leftrightarrow 2$ scattering in (5) comes from very small exchange momentum in $t \rightarrow 0$ or $u \rightarrow 0$ kinematic regimes, for which the incoming momenta only gets "deflected" by very small angle. If one uses this small angle approximation, then a rather neat kernel can be derived [16] :

$$\mathcal{C}_{2\leftrightarrow 2} = \xi \Lambda_s^2 \Lambda \frac{1}{p^2} \partial_p \left\{ p^2 \left[\frac{\partial f_p}{\partial p} + \frac{\alpha_s}{\Lambda_s} f_p \right] \right\}, \tag{8}$$

with $\xi = \frac{2N_c^2}{\pi} \int \frac{dq}{q}$ coming from the leading log contribution. The hard scale Λ and soft scale Λ_s in the above are defined via global integrals:

$$\Lambda \Lambda_s^2 / \alpha_s^2 = \int_0^\infty dp p^2 f_p (1+f_p) \equiv I_a\,, \tag{9}$$

$$\Lambda \Lambda_s / \alpha_s = \int_0^\infty dp p^2 (2f_p/p) \equiv I_b\,. \tag{10}$$

For later convenience we also introduce the Debye scale defined as [33, 34]

$$m_D^2 = -\alpha_s \int_0^\infty dp p^2 \partial f_p / \partial p = \Lambda \Lambda_s. \tag{11}$$

It is interesting to notice that in a weakly coupled thermal QGP one has the well-defined separation of scales, $\Lambda \sim T$, $m_D \sim gT$, $\Lambda_s \sim g^2 T$. The matter becomes strongly interacting when the scales "collapse" together. One way for that to happen is to have the system become really strongly coupled $g \to 1$ which likely will be accompanied by change of underlying degrees of freedom [35]. The other possibility, as in the case of Glasma, is when the system is highly off-equilibrium and overpopulated $f \sim 1/g^2$ — in this case all the scales also become of the same order $\Lambda \sim m_D \sim \Lambda_s \sim Q_s$ and make the system emerge as a strongly interacting matter.

Clearly, both the full form $C_{2\leftrightarrow 2}$ in (6) and the small angle approximation form in (8) conserve the energy as well as particle number, as they should. In addition the Bose-Einstein distribution $f_{BE} = 1/[e^{(p-\mu)/T} - 1]$ with any T and μ (in correspondence to the two conserved quantities) is the fixed point solution that makes both (6) and (8) vanish.

2.2 The $2 \leftrightarrow 3$ process

We now turn to the collision kernel from the $2 \leftrightarrow 3$ process as depicted in Fig.1. We denote the particle we are watching with momentum $\mathbf{p}$, the softest external momentum with $\mathbf{k}$, the exchange internal four-momentum with q^μ, and then the rest external momenta with $\mathbf{p}_{1,2,3}$. The $2 \leftrightarrow 3$ collision kernel can then be split into two pieces in which the particle $\mathbf{p}$ is on the two-particle side or three-particle side respectively (see Fig.1):

$$\begin{aligned}
\mathcal{C}_{2\leftrightarrow 3}[f_p] &= \mathcal{C}^a_{2\leftrightarrow 3} + \mathcal{C}^b_{2\leftrightarrow 3}, \qquad (12)\\
\mathcal{C}^a_{2\leftrightarrow 3} &= \frac{1}{N_g}\frac{1}{6}\int_{123k}\frac{1}{2E_p}|M_{1p\leftrightarrow 23k}|^2(2\pi)^4\delta^4(p+p_1-p_2-p_3-k)\\
&\quad \times[(1+f_p)(1+f_1)f_2f_3f_k - f_pf_1(1+f_2)(1+f_3)(1+f_k)],\\
\mathcal{C}^b_{2\leftrightarrow 3} &= \frac{1}{N_g}\frac{1}{4}\int_{123k}\frac{1}{2E_p}|M_{23\leftrightarrow 1kp}|^2(2\pi)^4\delta^4(p+p_1+k-p_2-p_3)\\
&\quad \times[(1+f_p)(1+f_1)(1+f_k)f_3f_2 - f_pf_1f_k(1+f_3)(1+f_2)], \qquad (13)
\end{aligned}$$

where the gluon labeled by k will be treated as the soft emitted or absorbed gluon. The factor $1/6$ counteracts the 6 equivalent permutations in $23k$ in process $1+p \leftrightarrow 2+3+k$ (see Fig. 1 left panel) and the factor $1/4$ counteracts the 4 equivalent permutations in $1k$ and 23 in process $2+3 \leftrightarrow 1+k+p$ (see Fig. 1 right panel). We note that the graphs in Fig. 1 are used to make the kinematics clear and it does not mean that only these two diagrams contribute: there are actually 25 different diagrams for $\mathcal{C}^a_{2\leftrightarrow 3}$ and 25 diagrams for $\mathcal{C}^b_{2\leftrightarrow 3}$. So the full matrix element square $|M_{1p\leftrightarrow 23k}|^2$ is obtained by calculating 25 Feynman diagrams and it contains 6 equivalent kinematic setups in accordance with 6 permutations in $23k$ (see Appendix A). We can then choose the kinematic setup corresponding to the Fig. 1 left panel, and multiply 6 to account other 5 kinematic setups. Similarly, we can fix the kinematics for $|M_{23\leftrightarrow 1kp}|^2$ as in the

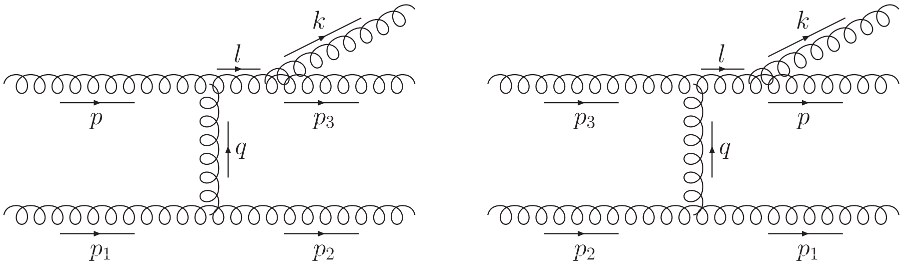

Figure 1: (Left) A typical Feynman diagram contributing to $\mathcal{C}^a_{2\leftrightarrow 3}$: $p+1 \leftrightarrow 2+3+k$. (Right) A typical Feynman diagram contributing to $\mathcal{C}^b_{2\leftrightarrow 3}$: $1+k+p \leftrightarrow 2+3$.

Fig. 1 right panel, and multiply 4 to get $\mathcal{C}^b_{2\leftrightarrow 3}$. Thus we get:

$$\begin{aligned}\mathcal{C}^a_{2\leftrightarrow 3} &= \frac{1}{N_g}\int_{123k}\frac{1}{2E_p}|M^a_{1p\to 23k}|^2(2\pi)^4\delta^4(p+p_1-p_2-p_3-k)\\ &\quad\times[(1+f_p)(1+f_1)f_2f_3f_k - f_pf_1(1+f_2)(1+f_3)(1+f_k)],\\ \mathcal{C}^b_{2\leftrightarrow 3} &= \frac{1}{N_g}\int_{123k}\frac{1}{2E_p}|M^b_{23\to 1kp}|^2(2\pi)^4\delta^4(p+p_1+k-p_2-p_3)\\ &\quad\times[(1+f_p)(1+f_1)(1+f_k)f_2f_3 - f_pf_1f_k(1+f_2)(1+f_3)], \quad (14)\end{aligned}$$

where $|M^{a,b}|^2$ are the matrix element square with the kinematics fixed according to Fig. 1. While the exact $2 \leftrightarrow 3$ matrix element square is known, it is very hard to be directly used in a kinetic approach. Following many previous studies involving this process [36, 37, 38, 39], we will use the so-called Gunion-Bertsch formula which is the collinear approximation and small angle approximation form of the exact matrix element and has been shown to give the dominant contribution in many cases. Leaving the technical details to the Appendix A, we quote the Gunion-Bertsch matrix element square which is at the leading order in soft q and k expansion:

$$\begin{aligned}|M^a_{1p\leftrightarrow 23k}|^2 &= 64g^6N_c^3N_g\frac{(p\cdot p_1)^3}{q^2(q-k)^2(p\cdot k)(p_1\cdot k)},\\ |M^b_{23\leftrightarrow 1kp}|^2 &= 64g^6N_c^3N_g\frac{(p_2\cdot p_3)^3}{q^2(q+k)^2(p_2\cdot k)(p_3\cdot k)}. \quad (15)\end{aligned}$$

Like in the $2 \leftrightarrow 2$ case, the matrix elements are dominated by the regime of very soft q and $\mathbf{k}$. We can thus further simplify the collision kernel using similar small angle approximation as in the elastic case. There is though additional subtlety as now there are two soft scales. In fact, as shown by the detailed analysis in Appendix B, the whole collision kernel can be separated into two pieces corresponding to contributions from different kinetic domains. (Note that both graphs in Fig. 1 contribute to each of these domains.) In the domain with $\mathbf{k}$ being the softest scale i.e. the ultra-soft emission and absorption, the $2 \leftrightarrow 3$ essentially reduces to an effective $2 \leftrightarrow 2$ scattering with a collinear splitting/merging, and the resulting contribution to the collision kernel becomes:

$$\begin{aligned}\mathcal{C}^{>}_{2\leftrightarrow 3} &\approx \frac{1}{N_g}\int_{12l}\frac{1}{2E_p}|M_{1p\to 2l}|^2(2\pi)^4\delta^4(p+p_1-p_2-l)\\ &\quad\times(g_p g_1 f_2 f_l - f_p f_1 g_2 g_l)\ \mathcal{D}(|q=p_1-p_2|),\end{aligned} \tag{16}$$

where the momentum labels l and q are as shown in Fig. 1, and we also introduced the term $\mathcal{D}(|q=p_1-p_2|)$ arising from the splitting function integration. For the above form, one can further simplify the effective $2\leftrightarrow 2$ part using small angle approximation as done in the elastic case. All the details are presented in Appendix B. On the other hand in the domain with q being the softest scale, the $2\leftrightarrow 3$ process effectively becomes a small angle $2\leftrightarrow 2$ scattering that brings one incoming particle slightly off-shell which undergoes a $1\leftrightarrow 2$ emission/combining. This part contributes the following to the collision kernel:

$$\begin{aligned}\mathcal{C}^{<}_{2\leftrightarrow 3} &= \frac{3g^6N_c^3}{16\pi^5}\int_0^\infty dp_1 p_1^2 h_1\int_{-1}^{1}\frac{dx}{1-x}\int_0^\infty\frac{dq}{q^3}\\ &\quad\times\int_0^{z_c}\frac{dz}{z}\Big\{\left[g_p f_{(1-z)p}f_{zp}-f_p g_{(1-z)p}g_{zp}\right]\\ &\qquad+\frac{1}{(1-z)^4}\left[g_p g_{zp/(1-z)}f_{p/(1-z)}-f_p f_{zp/(1-z)}g_{p/(1-z)})\right]\Big\}\end{aligned} \tag{17}$$

Note in the z-integration we introduce the upper cut $z<z_c$: physically this is because the $\mathcal{C}^{<}_{2\leftrightarrow 3}$ is from the domain with k being the softest external momentum so the $k<p$ condition would require $z_c<1/2$. In both kernels above, a number of infrared divergences appear. We will use the Debye scale m_D as the infrared cut, e.g. $\int dq/q^3 \approx 1/m_D^2 = 1/(\Lambda\Lambda_s)$. We will also treat all leading logs as order one constant. Again more detailed discussions are included in the Appendix B. Lastly, one can show that the inelastic kernel conserves energy while not particle number, and the fixed point solution (i.e. the equilibrium distribution) is the Bose-Einstein distribution *without* chemical potential $f_{BE}=1/(e^{p/T}-1)$.

2.3 The final kinetic equation

Finally we combine the $\mathcal{C}_{2\leftrightarrow 2}$ and $\mathcal{C}_{2\leftrightarrow 3}$ kernels, and the final kinetic equation under small angle approximation and collinear approximation reads

$$\mathcal{D}_t f_p = \mathcal{C}^{\text{eff}}_{2\leftrightarrow 2}[f_p]+\mathcal{C}^{\text{eff}}_{1\leftrightarrow 2}[f_p], \tag{18}$$

where

$$\mathcal{C}^{\text{eff}}_{2\leftrightarrow 2}=\mathcal{C}_{2\leftrightarrow 2}+\mathcal{C}^{>}_{2\leftrightarrow 3},\quad \mathcal{C}^{\text{eff}}_{1\leftrightarrow 2}=\mathcal{C}^{<}_{2\leftrightarrow 3}. \tag{19}$$

The expression for $\mathcal{C}^{\text{eff}}_{2\to 2}$ is

$$\mathcal{C}^{\text{eff}}_{2\leftrightarrow 2} = \xi\alpha_s^2\,(1+D)\,I_a\frac{1}{p^2}\partial_p\left\{p^2\left[\frac{\partial f_p}{\partial p}+\frac{I_b}{I_a}f_p\right]\right\}, \tag{20}$$

with $D \sim \hat{O}(1)$ parameterizing the contribution from $\mathcal{C}^{>}_{2\leftrightarrow 3}$ to effective $2 \leftrightarrow 2$. The expression for $\mathcal{C}^{\text{eff}}_{1\leftrightarrow 2}$ is

$$\begin{aligned}\mathcal{C}^{\text{eff}}_{1\leftrightarrow 2} \quad &= \quad \xi\, \alpha_s^2\, R\, \frac{I_a}{I_b} \bigg\{ \int_0^{z_c} \frac{dz}{z} \left[g_p f_{(1-z)p} f_{zp} - f_p g_{(1-z)p} g_{zp} \right] \\ &\qquad + \int_0^{z_c} \frac{dz}{(1-z)^4 z} \left[g_p g_{zp/(1-z)} f_{p/(1-z)} - f_p f_{zp/(1-z)} g_{p/(1-z)} \right] \bigg\} \end{aligned} \tag{21}$$

where the constant $R \sim \hat{O}(1)$ parameterizes the relative ratio of the order one constants between the elastic and inelastic kernels and the cut z_c in z-integration should be small to be consistent with the kinematics $k < p$. The expressions for D and R can be found in Appendix B.

A few comments are in order here:
1) The kernel (20) conserves energy and particle number with fixed point solution $f_{BE} = 1/[e^{(p-\mu)/T} - 1]$, while the kernel (21) only conserves energy with fixed point solution $f_{BE} = 1/[e^{p/T} - 1]$, so the total kernel (18) conserves only energy and the equilibrium solution should be $f_{BE} = 1/[e^{p/T} - 1]$ without any chemical potential which is different from the pure elastic case;
2) In the near equilibrium case with $f \sim \hat{o}(1)$, $I_a \sim T^3$ and $I_b \sim T^2$, the elastic collision rate scales as $\sim \alpha_s^2 T$ and the inelastic rate scales also as $\sim \alpha_s^2 T$ so they are at parametrically the same order;
3) In the glasma-like overpopulated case with $f \sim \hat{o}(1/\alpha_s)$, $I_a \sim Q_s^3/\alpha_s^2$ and $I_b \sim Q_s^2/\alpha_s$, the elastic collision rate scales as $\sim Q_s$ and the inelastic rate scales also as $\sim Q_s$ so again they are at parametrically the same order.
We therefore see that the effect of the inelastic collision is parametrically as important as the elastic one both near and far from equilibrium, and including the inelastic collision qualitatively changes the ultimate equilibrium solution. It is clear that even starting from highly overpopulated initial condition, eventually there will be no chemical potential nor any condensate in the final thermal distribution with the presence of inelastic collision. However, the very important question that has not been understood, is how the inelastic collision will affect the transient dynamical off-equilibrium condensation driven by the pure elastic evolution starting from initial high overpopulation. Will the system still reach the onset of such condensation? Will the inelastic collision speed up, delay, or completely eliminate such an onset? We will address these questions by numerically solving the above kinetic equations.

3 Numerical Study of the Kinetic Evolution

In this section, we numerically solve the kinetic equation (18), starting with a Glasma-type initial condition as follows:

$$f(p, t = 0) = f_0\, \theta(Q_s - p) \tag{22}$$

with Q_s the saturation scale. We use Q_s as unit for all momenta/enegy etc and use $1/Q_s$ as unit for time. As studied in [16], with a given initial occupation f_0, the overpopulation parameter is $n\epsilon^{-3/4} = f_0^{1/4}\, 2^{5/4}/3\pi^1/2$ and when $f_0 > f_0^c \approx 0.154$, the system is overpopulated as compared with the Stefan-Boltzmann limit and the system will reach onset of condensation when there is only elastic collision. For simplicity we fix the initial occupation $f_0 = 1$ which is in the overpopulated regime. Note that for the the constant $\xi\alpha_s^2$ can be absorbed by a redefinition of time variable, $t \to (\xi\alpha_s^2)t$ which we will use from now on. We therefore are left with three parameters, R, D, and z_c. The inelastic contribution will increase with increasing R and a while the elastic will increase with increasing D. We will study the effect of inelastic collision by comparison with pure elastic case ($R = 0$ versus $R \neq 0$) and by varying the strength of the inelastic contribution. In passing let us also mention that we have studied the case with only inelastic collision, and in that case indeed the system simply thermalizes into equilibrium Bose-Einstein distribution with temperature to be the supposed value required by energy conservation and without any chemical potential.

3.1 From overpopulation toward onset of condensation

Let us first briefly summarize the kinetic evolution from overpopulation toward onset of condensation in the purely elastic case, as reported in [16, 31, 32]. The elastic kernel can be re-written in terms of flux as

$$C_{2\leftrightarrow 2} = -\frac{1}{p^2}\partial_p(p^2\, S(p)),\ \ S(p) \equiv -\left[I_a \partial_p f_p + I_b f_p(1+f_p)\right] \tag{23}$$

The strong overpopulation leads to a particle flux cascade toward the infrared regime. Analysis of the small p regime shows that it will quickly develop a local thermal form $f^*(p) = 1/[e^{(p-\mu^*)/T^*} - 1]$ with $T^* = I_a/I_b$, and the incoming flux will drive the (negative) μ^* to eventually vanish and reach the onset of a dynamical condensation. This picture is numerically verified in great details in [16]. Our discussion of the onset of condensation will stay in this picture (as the elastic term is still present and its flux drives the small p behavior) and we will study how the inelastic process modifies it.

Starting with the overpopulated initial condition (22) we have numerically evolved the kinetic equations (18), (20), and (21) with given set of parameters. Shown in Fig. 2 is the solution with $R = 1$. In Fig. 2 left we show the distribution function f_p at different time moments, and one can see that even with the presence of inelastic term, the small p part of the distribution is quickly filled up and becomes a local thermal form $f^*(p) = 1/[e^{(p-\mu^*)/T^*} - 1]$ despite that the distribution in the wide range of (bigger) momentum region is still far from equilibrium shape, and the small p part becomes steeper and steeper with time (meaning decreasing $|\mu^*|$). In Fig. 2 right we show the corresponding flux $S(p)$ from the elastic kernel. Again the flux behaves very similarly to the purely elastic case: one see a linear behavior at small p, $S \propto -p$ and eventually upon onset of condensation the flux diverges (see the blue curve near $p = 0$).

To get an intuitive idea of the contribution of the inelastic kernel, we plot the $C_{1\leftrightarrow 2}$ and $p^2 C_{1\leftrightarrow 2}$ in Fig. 3. One can see that the kernel is large and

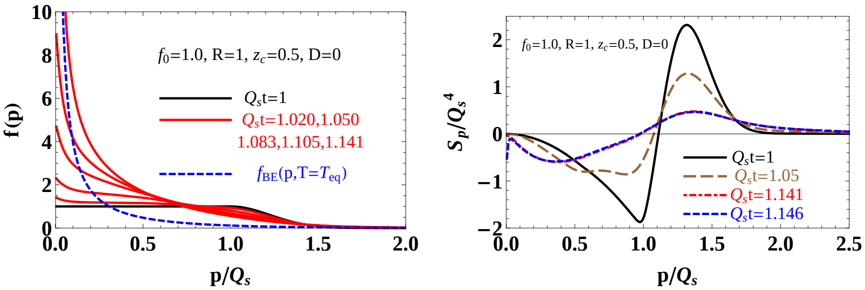

Figure 2: (Left) The distribution function $f(p)$ at different time moments during evolution; (Right) The flux $S(p)$ defined in elastic kernel at different time moments during evolution.

positive at small p, small and positive at large p, while negative at intermediate p. This could be qualitatively understood: significant number of particles with intermediate momenta will merge toward high momenta and split toward low momenta that will fill up UV and IR region while decrease the occupation at intermediate momenta. We also notice that upon onset (the blue dashed curve in the right panel) the inelastic kernel near $p = 0$ shows a divergent behavior in consistency with the elastic flux behavior.

One can directly examine the locally determined T^* and μ^* (see [16] for details) at each time moment during the evolution: these results are shown in Fig. 4. Here we also compare the results for different strength of the inelastic collision $R = 0, 0.1, 1, 10$ (noting that the $R = 0$ case corresponds to purely elastic collision). In all cases we can see that the local "chemical potential" μ^* decreases rather rapidly toward zero. We also show the distribution $f(p)$ at the smallest grid point in our calculation $p = 0.005Q_s$ as a function of time in Fig. 5, which shows very rapid increase of the occupation in consistence with the vanishing of μ^*. What is most striking is that with increase values of R this evolution toward the onset of condensation $\mu^* \to 0$ becomes faster and faster. The $R = 1$ case is already much faster than the purely elastic case. This is to say, contrary to expectation that the inelastic process may "kill" the strong overpopulation quickly, the existence of inelastic collision actually **speeds up** significantly the process of populating the infrared regime and building up a local thermal form with vanishing μ^*, which when combined with the structure of elastic kernel will then lead to the onset of condensation.

3.2 Small p analysis of the inelastic kernel

To understand better the influence of inelastic collision on the small p region, let us examine the kernel (21) for $p \to 0$ limit before the onset of condensation. Provided that $f_0 = f(p = 0) < \infty$ and that its derivatives with respect to p at $p = 0$ is also finite, we can have the expansion $f(p \to 0) \approx f_0 + f_0' p + ...$ If we look at a small enough p regime, then all the involved momenta $(p, zp, (1 - z)p, p/(1 - z), pz/(1 - z))$ in the kernel (21) can be considered small and we can

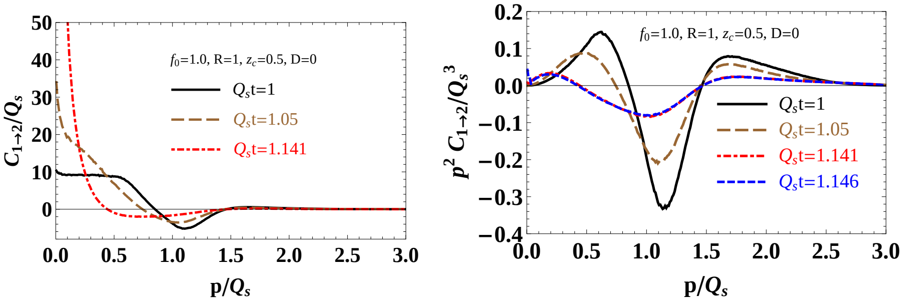

Figure 3: The inelastic kernel $C_{1\leftrightarrow 2}(p)$ (Left) and $p^2C_{1\leftrightarrow 2}(p)$ (Right) at different time moments during evolution.

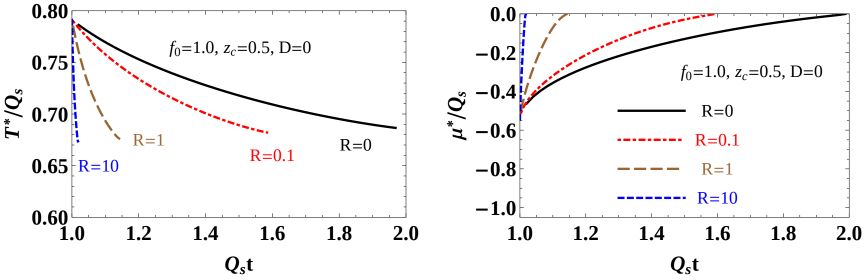

Figure 4: The local thermal form parameters T^* (Left) and μ^* (Right) as functions of time for different values of parameter R.

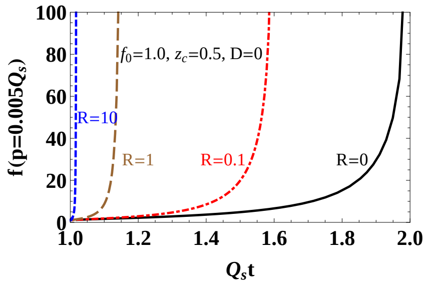

Figure 5: The occupation at the smallest grid point $f(p = 0.005Q_s)$ as a function of time for different values of parameter R.

use the expansion for them. This leads to

$$\mathcal{C}^{\rm eff}_{1\leftrightarrow 2}(p\to 0) \to R\frac{I_a}{I_b}\left[A_0 f_0(1+f_0) + A_1 f_0'(1+2f_0)\,p + \hat{O}(p^2)\right], \tag{24}$$

where we have introduced the constants

$$\begin{aligned} A_0 &= \ln\frac{1}{1-z_c} + \frac{1}{6}\frac{z_c(11z_c^2 - 27z_c + 18)}{(1-z_c)^3}, \\ A_1 &= \ln\frac{1}{1-z_c} - \frac{1}{12}\frac{z_c(25z_c^3 - 88z_c^2 + 108z_c - 48)}{(1-z_c)^4}. \end{aligned} \tag{25}$$

All these A's are positive for $0 < z_c < 1$. Clearly for sufficiently small p the leading term in the inelastic kernel $\sim f_0(1+f_0)A_0$ is *always positive* and becomes bigger and bigger with increasing f_0 (which is a kind of "self-amplification"). This will tend to increase the particle number near $p = 0$ very rapidly and the effect becomes stronger with increasing values of R, which explains the behavior seen in Fig. 5.

Physically this behavior may be understood in two ways. First note that the inelastic kernel has its fixed point to be $1/(e^{p/T} - 1)$ which at small p is $\sim 1/p$ so as long as $f(p = 0)$ is finite yet the inelastic kernel will try to fill it up toward $1/p$. Second, this is also related to the Boson nature: if all involved particles are from small p, then the merging rate is like $\sim f_0^2(1 + f_0)$ while the splitting rate is like $\sim f_0(1 + f_0)^2$ so the splitting "wins" due to Bose enhancement for the final state particles and it increases particle number at small p. To conclude, the inelastic kernel contribution is always positive at very small p and it will catalyze and speed up the onset of a Bose condensation (which itself is driven by the elastic term at $\mu^* \to 0$).

3.3 Change of particle number from inelastic kernel

While the inelastic kernel always increases the occupation at sufficiently small p, it may still decrease the the total particle number. Indeed as shown in Fig. 6 (left panel), the total particle number decreases when $R > 0$, and it decreases more rapidly for larger R.

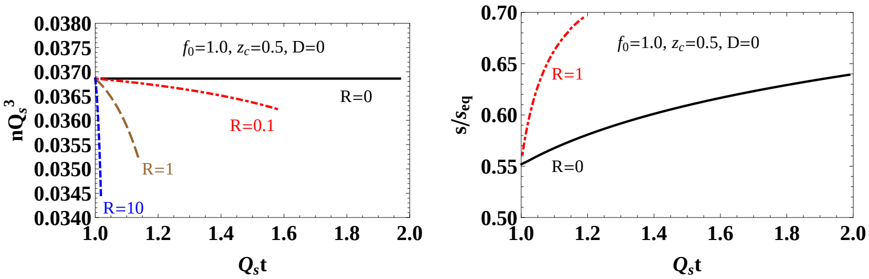

Figure 6: (Left) The particle number density as a function of time for different values of parameter R. (Right) The entropy density as a function of time for $R = 1$ and $R = 0$.

To understand the change of particle number $n = \int_p f(p)$, one can integrate the two sides of the kinetic equation (18) and obtain

$$\begin{aligned}\partial_t n(t) &= R\frac{I_a}{2\pi^2 I_b}\int dpp^2\int_0^{z_c}\frac{dz}{1-z}\left[f_p g_{(1-z)p} g_{zp} - g_p f_{(1-z)p} f_{zp}\right] \\ &= R\frac{I_a}{2\pi^2 I_b}\int dpp^2\int_0^{z_c}\frac{dz}{1-z}\left[f_p + f_p f_{(1-z)p} + f_p f_{zp} - f_{(1-z)p} f_{zp}\right]. \end{aligned} \tag{26}$$

From the above one can see the for the region $z \to 0$ the leading order in the z-integrand becomes $\sim f_p(1+f_p)$ and the contribution is positive, i.e. increasing particle number. For general z, the z-integrand can be rewritten as

$$\partial_t n(t) = R\frac{I_a}{2\pi^2 I_b}\int dpp^2\int_0^{z_c}\frac{dz}{1-z}\left[f_p(1+f_p) - (f_{(1-z)p} - f_p)(f_{zp} - f_p)\right]. \tag{27}$$

We see that for not too small z, the momenta zp, $(1-z)p$ become well separated from p and the second term in the above integrand becomes important and its contribution is negative which decreases the particle number.

In Fig. 6 (right panel) we also show the entropy density as a function of time and compare the case with $R = 1$ and the purely elastic case with $R = 0$. One can see that with inelastic collision included, the entropy density increases much faster. That is, the inelastic process tends to accelerate the thermalization.

3.4 Dependence on the parameter z_c

Finally we study the dependence on the parameter z_c which is the kinematic cut to make sure the validity of the approximations used for the matrix element. Generally speaking, with larger z_c we include more effects from the inelastic process. To see how the results depend on z_c, we fix other parameters and compare the results for different choices of z_c. In Fig. 7, we show the local thermal form parameters T^* (left panel) and μ^* (right panel) as functions of time for $z_c = 0.2, 0.5, 0.8$ respectively. In Fig. 8, we show the occupation at the smallest grid point (left panel) and the total particle number (right panel)

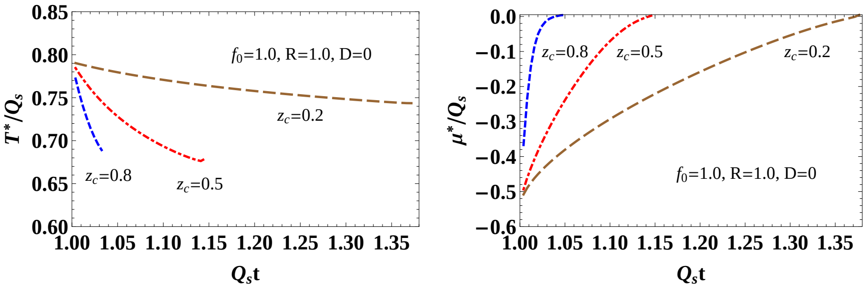

Figure 7: The local thermal form parameters T^* (Left) and μ^* (Right) as functions of time for $z_c = 0.2, 0.5, 0.8$ respectively.

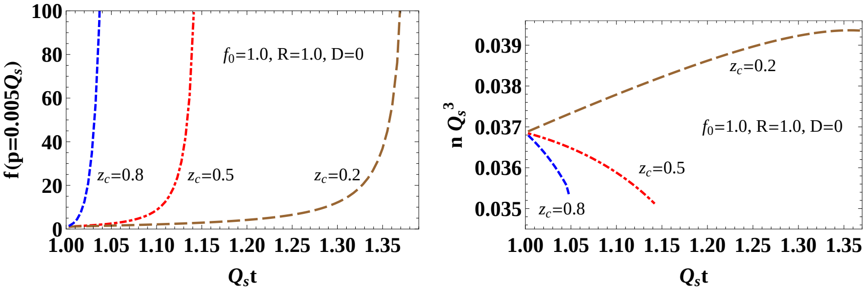

Figure 8: The occupation at the smallest grid point $f(p = 0.005Q_s)$ (Left) and the particle number density (Right) as functions of time for $z_c = 0.2, 0.5, 0.8$ respectively

as functions of time for $z_c = 0.2, 0.5, 0.8$ respectively. From the plots we can see that indeed with larger z_c the f_0 increases faster and μ^* vanishes faster as expected for stronger inelastic effect. For the particle number, the case with $z_c = 0.2$ actually has n increasing with time, which can be understood fro m the analysis in the previous subsection. The particle number in both $z_c = 0.5$ and $z_c = 0.8$ cases drops with time and does so faster for larger z_c. In passing let us mention that we have also studied the dependence on the parameter D: basically increasing D will enhance the effect from elastic collision and also speed up the thermalization in general, as well as reach onset of condensation at earlier times compared with $D = 0$ case.

4 Conclusion

In summary, we have studied the kinetic evolution of a highly overpopulated system starting from Glasma-type initial condition with the presence of both elastic and inelastic collisions. Using the Gunion-Bertsch formula for the $2 \leftrightarrow 3$ matrix element, we have derived the inelastic collision kernel under the collinear and small angle approximations. Putting together the inelastic kernel together with the previously obtained elastic kernel, we have then numerically solved the kinetic evolution for varied choices of parameters. Our main finding is that the inelastic process has two effects: globally changing (mostly reducing) the total particle number, while locally at small p always filling up the infrared regime extremely quickly. The latter effect is shown both from numerics and by analytic analysis. This effect significantly speeds up the emergence of local thermal form near $p = 0$ and the vanishing of local "chemical potential" μ^* as previously found in the purely elastic collision case to lead to the onset of dynamical Bose condensation. Therefore in our present approach of including the inelastic scattering, we conclude that, contrary to some previously discussed expectations about the role of number non-conserving processes, the inelastic collision actually helps to build up the local "critical form" $\sim 1/p$ much faster and catalyzes the onset of condensation in the overpopulated Glasma.

Acknowledgements

The authors are particularly grateful to L. McLerran for very helpful discussions. J.L. also thanks J.-P. Blaizot, F. Gelis, and R. Venugopalan for collaborations and communications that motivated and benefited this work. J.L. acknowledges the RIKEN BNL Research Center for partial support.

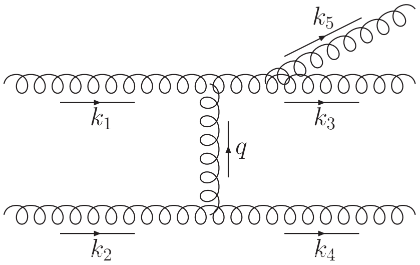

Figure 9: A typical Feynman diagram for $M_{2\leftrightarrow 3}$.

Appendix

A $gg \to ggg$ matrix element square

The invariant $gg \to ggg$ matrix element square summed over all final states and also summed over all initial states is computed by considering 25 different diagrams [40]. We quote it here:

$$\begin{aligned}|M_{2\to 3}|^2 &= g^6 N_c^3 N_g \frac{\mathcal{N}}{\mathcal{D}}[(12345)+(12354)+(12435)+(12453)+(12534)\\ &\quad +(12543)+(13245)+(13254)+(13524)+(14235)+(14325)],\end{aligned} \tag{28}$$

where $N_c = 3$ and $N_g = 2(N_c^2-1)$,

$$\begin{aligned}\mathcal{N} &= (12)^4+(13)^4+(14)^4+(15)^4+(23)^4+(24)^4\\ &\quad +(25)^4+(34)^4+(35)^4+(45)^4,\\ \mathcal{D} &= (12)(13)(14)(15)(23)(24)(25)(34)(35)(45),\\ (ijklm) &= (ij)(jk)(kl)(lm)(mi),\\ (ij) &\equiv k_i \cdot k_j.\end{aligned} \tag{29}$$

$|M_{2\to 3}|^2$ is completely symmetry in $k_i, i = 1-5$, so let's take k_1 and k_2 as the hard momenta in the entrance channel, k_3 and k_4 as the hard momenta in the exit channel, and k_5 as the emitted soft gluon. We also denote the exchanging momentum as $q = k_2 - k_4$. A typical Feynman diagram illuminating this set-up is shown in Fig. 9.

Define the Mandelstam variables as [41, 42]:

$$\begin{aligned}s = (k_1+k_2)^2 = 2(12),\ t = (k_1-k_3)^2 = -2(13),\ u = (k_1-k_4)^2 = -2(14),\\ s' = (k_3+k_4)^2 = 2(34),\ t' = (k_2-k_4)^2 = -2(24),\ u' = (k_2-k_3)^2 = -2(23).\end{aligned}$$

In addition, the following relations involving k_5 hold:

$$(15) = \frac{s+t+u}{2},\ (25) = \frac{s+t'+u'}{2},\ (35) = \frac{s+t'+u}{2},\ (45) = \frac{s+t+u'}{2}.$$

In terms of the Mandelstam variables, $|M_{2\to 3}|^2$ can be written as

$$\begin{aligned}
|M_{2\to 3}|^2 &= 32g^6N_c^3N_g\mathcal{N}\Big[\frac{1}{s'(s+u+t)(s+u'+t')}\Big(\frac{1}{tt'}+\frac{1}{uu'}\Big) \\
&\quad +\frac{1}{s(s+u'+t)(s+u+t')}\Big(\frac{1}{tt'}+\frac{1}{uu'}\Big) \\
&\quad -\frac{1}{t'(s+u+t)(s+u+t')}\Big(\frac{1}{ss'}+\frac{1}{uu'}\Big) \\
&\quad -\frac{1}{t(s+u'+t)(s+u'+t')}\Big(\frac{1}{ss'}+\frac{1}{uu'}\Big) \\
&\quad -\frac{1}{u'(s+u+t)(s+u'+t)}\Big(\frac{1}{tt'}+\frac{1}{ss'}\Big) \\
&\quad -\frac{1}{u(s+u+t')(s+u'+t')}\Big(\frac{1}{tt'}+\frac{1}{ss'}\Big)\Big], \qquad (30)
\end{aligned}$$

where

$$\begin{aligned}
\mathcal{N} &= \frac{1}{16}[s^4+t^4+u^4+s'^4+t'^4+u'^4+(s+u+t)^4 \\
&\quad +(s+u'+t')^4+(s+t'+u)^4+(s+t+u')^4].
\end{aligned}$$

Assume $q=k_2-k_4$ is small as well as k_5. Then t,t' are small, while s,s',u,u' are large, and $-u\to -u'\to s'\to s$. We do an expansion for $|M|^2$ and keep only leading and subleading order terms in q and k_5. First,

$$\begin{aligned}
s' &= (k_1+k_2-k_5)^2 = s-2(k_1+k_2)\cdot k_5+O(k_5^2), \\
u &= -s+2k_1\cdot k_5+O(q^2), \\
u' &= -s+2k_2\cdot k_5+O(q-k_5)^2, \\
t &= (q-k_5)^2, \\
t' &= q^2.
\end{aligned}$$

Second,

$$\begin{aligned}
k_2\cdot(k_4+q)=0 \Rightarrow k_2\cdot q = -k_2\cdot k_4 = \frac{1}{2}(k_2-k_4)^2 = \frac{1}{2}q^2, \\
t-t'=-2q\cdot k_5 \Rightarrow -2q\cdot k_2-2k_1\cdot(q-k_5) = 2k_2\cdot k_4-2k_1\cdot k_3 = t-t' = -2q\cdot k_5 \\
\Rightarrow k_1\cdot(k_5-q) = \frac{q^2}{2}-q\cdot k_5.
\end{aligned}$$

Then $\mathcal{N}$ and $|M_{2\to 3}|^2$ can be simplified as

$$\begin{aligned}
\mathcal{N} &= \frac{s^4}{4} - s^3(k_2\cdot k_5 + k_1\cdot k_5) + O(k_5^2, q^2, k_5\cdot q), && (31)\\
|M_{2\to 3}|^2 &= 32g^6N_c^3N_g\frac{\mathcal{N}}{tt'}\Big[\frac{1}{s'(s+u+t)(s+u'+t')} + \frac{1}{s(s+u'+t)(s+u+t')}\\
&\quad -\frac{1}{u'(s+u+t)(s+u'+t)} - \frac{1}{u(s+u+t')(s+u'+t')}\Big] + O\left(\frac{t}{s}\right)\\
&= 32g^6N_c^3N_g\frac{\mathcal{N}}{tt'}\frac{s+(k_1+k_2)\cdot k_5}{s^2(k_1\cdot k_5)(k_2\cdot k_5)} + O(k_5,q)^2\\
&= 8g^6N_c^3N_g\frac{s^2}{tt'}\frac{s-3(k_1+k_2)\cdot k_5}{(k_1\cdot k_5)(k_2\cdot k_5)} + O(k_5,q)^2\\
&= 32g^6N_c^3N_g\frac{(k_1\cdot k_2)^2}{q^2(q-k_5)^2}\frac{2k_1\cdot k_2 - 3(k_1+k_2)\cdot k_5}{(k_1\cdot k_5)(k_2\cdot k_5)} + O(k_5,q)^2. && (32)
\end{aligned}$$

In the center of mass frame of k_1 and k_2, it goes to

$$\begin{aligned}
|M_{2\to 3}^{c.m.}|^2 &\approx |M_{\rm GB}|^2\left(1-3\frac{|\mathbf{k}_5|}{\sqrt{s}}\right)\left(1+\frac{q_0^2-\mathbf{q}_\parallel^2}{\mathbf{q}_\perp^2}\right)\left(1+\frac{(q_0-k_{50})^2-(\mathbf{q}_\parallel-\mathbf{k}_{5\parallel})^2}{(\mathbf{q}_\perp-\mathbf{k}_{5\perp})^2}\right)\\
&\approx |M_{\rm GB}|^2\left(1-3\frac{|\mathbf{k}_{5\perp}|}{\sqrt{s}}\right), && (33)
\end{aligned}$$

where $\mathbf{q}_\parallel = (\mathbf{q}\cdot\mathbf{v}_1)\mathbf{v}_1$ and

$$|M_{\rm GB}|^2 = 32g^6N_c^3N_g\frac{s^2}{\mathbf{q}_\perp^2(\mathbf{q}_\perp-\mathbf{k}_{5\perp})^2\mathbf{k}_{5\perp}^2} \tag{34}$$

is the Gunion-Bertsch formula. We used the fact that, in any frame, $q_0^2 = (\mathbf{v}_2\cdot\mathbf{q})^2 + O(q_\perp^2 q_0)$ and $(q_0-k_{50})^2 = (\mathbf{v}_1\cdot(\mathbf{q}-\mathbf{k}_5))^2 + O(q_\perp - k_{5\perp})^2(q_0-k_{50})$ for soft q and k_5. Thus, Gunion-Bertsch formula is the leading order amplitude in soft q and k expansion; and Eq. (32) is the amplitude including both the leading (Gunion-Bertsch) and the subleading order terms. Higher order terms can also be obtained, but we won't use them. Note that one can naively boosts the Gunion-Bertsch formula from the center of mass frame to a general frame by using the replacements $\mathbf{k}_{5\perp}^2 \to 4(k_1\cdot k_5)(k_2\cdot k_5)/s$, $\mathbf{q}_\perp^2 \to 4(k_1\cdot k_4)(k_2\cdot k_4)/s$, and $(\mathbf{q}_\perp-\mathbf{k}_{5\perp})^2 \to 4(k_1\cdot k_3)(k_2\cdot k_3)/s$. The result coincides with Eq. (32) at leading order but not at next to leading order in soft q and k_5 expansion:

$$|M_{\rm GB}|^2 = 16g^6N_c^3N_g\frac{(k_1\cdot k_2)^5}{(k_1\cdot k_3)(k_2\cdot k_3)(k_1\cdot k_4)(k_2\cdot k_4)(k_1\cdot k_5)(k_2\cdot k_5)}. \tag{35}$$

B The collision kernel $\mathcal{C}_{2\to 3}$ at collinear approximation

The collision kernel $\mathcal{C}_{2\to 3}$ has a very complicated structure, in this section, we simplify it by taking the collinear approximation, i.e., $\mathbf{v}_k \simeq \mathbf{v}_1$ or $\mathbf{v}_k \simeq \mathbf{v}_p$.

We thus rewrite the collision kernels $\mathcal{C}^a_{2\to 3}$ and $\mathcal{C}^b_{2\to 3}$ as (We denote $1+f_i$ by g_i)

$$\begin{aligned}
\mathcal{C}^a_{2\to 3} &= \frac{1}{N_g}\int_{123kl}\frac{2E_l}{2E_p}\int\frac{d^4q}{(2\pi)^4}\int\frac{dl_0}{2\pi}(2\pi)^4\delta^4(p+q-l)(2\pi)^4\delta^4(p_1-q-p_2) \\
&\quad \times(2\pi)^4\delta^4(l-k-p_3)|M^a_{1p\to 23k}|^2(g_pg_1f_2f_3f_k-f_pf_1g_2g_3g_k), \\
\mathcal{C}^b_{2\to 3} &= \frac{1}{N_g}\int_{123kl}\frac{2E_l}{2E_p}\int\frac{d^4q}{(2\pi)^4}\int\frac{dl_0}{2\pi}(2\pi)^4\delta^4(p+q-l)(2\pi)^4\delta^4(p_1-q-p_2) \\
&\quad \times(2\pi)^4\delta^4(l+k-p_3)|M^b_{23\to 1pk}|^2(g_pg_1g_kf_2f_3-f_pf_1f_kg_2g_3), \qquad (36)
\end{aligned}$$

where we introduced two auxiliary integrations over l and q, the kinematics is shown in Fig. 1.

First, it is easy to show that, under small angle approximation,

$$\begin{aligned}
q_0 &\simeq \mathbf{q}\cdot\mathbf{v}_1-\frac{\mathbf{q'}^2_\perp}{2E_1} \\
&\simeq E_k+(\mathbf{q}-\mathbf{k})\cdot\mathbf{v}_p+\frac{(\mathbf{q}_\perp-\mathbf{k}_\perp)^2}{2E_p}, \qquad (37) \\
l_0 &\simeq E_l+E_k-\mathbf{k}\cdot\mathbf{v}_l+\frac{\mathbf{k''}^2_\perp}{2E_l} \\
&\simeq E_p+q_0, \qquad (38) \\
\mathbf{v}_l &\simeq \mathbf{v}_p+\frac{\mathbf{q}_\perp}{E_p}-\frac{\mathbf{q}^2_\perp}{2E^2_p}\mathbf{v}_p+\frac{(\mathbf{q}\cdot\mathbf{v}_p)^2}{E^2_p}\mathbf{v}_p-\frac{\mathbf{q}\cdot\mathbf{v}_p}{E^2_p}\mathbf{v}_q, \qquad (39)
\end{aligned}$$

where $\mathbf{q}_\perp=\mathbf{q}-\mathbf{q}\cdot\mathbf{v}_p\mathbf{v}_p$, $\mathbf{k}_\perp=\mathbf{k}-\mathbf{k}\cdot\mathbf{v}_p\mathbf{v}_p$, $\mathbf{q}'_\perp=\mathbf{q}-\mathbf{q}\cdot\mathbf{v}_1\mathbf{v}_1$, and $\mathbf{k''}_\perp=\mathbf{k}-\mathbf{k}\cdot\mathbf{v}_l\mathbf{v}_l$.

Second, if $k<q$, then, under collinear approximation, $\mathbf{v}_k$ is either nearly parallel to $\mathbf{v}_p$ or $\mathbf{v}_1$. For $\mathbf{v}_k\simeq\mathbf{v}_1$, $q\cdot k=|\mathbf{k}|(q_0-\mathbf{q}\cdot\mathbf{v}_k)\simeq|\mathbf{k}|[q_0-\mathbf{q}\cdot\mathbf{v}_1+\mathbf{q}\cdot(\mathbf{v}_1-\mathbf{v}_k)]\sim-|\mathbf{k}|\mathbf{q'}^2_\perp/E_1+|\mathbf{k}||\mathbf{q}|\theta_{1k}\ll q^2$; For $\mathbf{v}_k\simeq\mathbf{v}_p$, $q\cdot k=|\mathbf{k}|(|\mathbf{k}|-\mathbf{k}\cdot\mathbf{v}_l)\sim|\mathbf{k}|^2\theta^2_{kp}+|\mathbf{k}|\mathbf{q}^2_\perp/(2E_p)+|\mathbf{k}||\mathbf{q}|\theta_{kp}\ll q^2$. Thus in the small angle plus collinear approximation, if $k<q$, we can approximate the amplitude $|M^a_{1p\to 23k}|^2$ as

$$|M^a_{1p\to 23k}|^2 = 64g^6N_c^3N_g\frac{(p\cdot p_1)^3}{(q^2)^2(p\cdot k)(p_1\cdot k)}. \qquad (40)$$

For $|M^b_{23\to 1pk}|^2$, up to q^2 order, we can neglect $q\cdot k$ in the denominator and $q\cdot p$ and $q\cdot p_1$ in the numerator,

$$\begin{aligned}
|M^b_{23\to 1kp}|^2 &= 64g^6N_c^3N_g\frac{[(p_1+q)\cdot(p+k-q)]^3}{q^2(q+k)^2[(p+k-q)\cdot k][(p_1+q)\cdot k]} \\
&\approx 64g^6N_c^3N_g\frac{[(p_1+q)\cdot(p-q)]^3}{(q^2)^2[(p-q)\cdot k][(p_1+q)\cdot k]} \\
&\approx 64g^6N_c^3N_g\frac{(p_1\cdot p)^3}{(q^2)^2(p\cdot k)(p_1\cdot k)} \\
&= |M^a_{1p\to 23k}|^2. \qquad (41)
\end{aligned}$$

Third, if $k > q$, under the collinear approximation, for $\mathbf{v}_k \simeq \mathbf{v}_1$, $q \cdot k \sim -|\mathbf{k}|\mathbf{q'}_\perp^2/E_1 + |\mathbf{k}||\mathbf{q}|\theta_{1k} \ll q^2$ because $\theta_{1k} \ll |\mathbf{q}'|_\perp/E_1$; For $\mathbf{v}_k \simeq \mathbf{v}_p$, $q \cdot k \sim |\mathbf{k}|^2\theta_{kp}^2 + |\mathbf{k}|\mathbf{q}_\perp^2/(2E_p) + |\mathbf{k}||\mathbf{q}|\theta_{kp} \ll q^2$ because $\theta_{kp} \ll |\mathbf{p}_\perp|/E_p$. Thus the collinear approximation can simplify the amplitude even when $k > q$:

$$\begin{aligned} |M^a_{1p\to 23k}|^2 &= 64g^6N_c^3N_g\frac{(p\cdot p_1)^3}{(q^2)^2(p\cdot k)(p_1\cdot k)} \\ |M^b_{23\to 1kp}|^2 &= 64g^6N_c^3N_g\frac{[(p+k)\cdot p_1]^3}{(q^2)^2(p\cdot k)(p_1\cdot k)}. \end{aligned} \tag{42}$$

Fourth, the whole kinematic (phase) space can be separated into two parts: one for $k < q$ and the other for $q < k$. We would expect that at kinematic region with $k < q$, the $2 \to 3$ process may be regarded as a $2 \to 2$ "hard" process with one additional "soft" gluon emitted or absorbed by one of the "hard" gluons; with $q < k$ the $2 \to 3$ process can be regarded as an effective $1 \to 2$ process with a spectator gluon joined to make the effective $1 \to 2$ amplitude nonzero (the amplitude of $1 \to 2$ process is zero for massless gluons). Thus we separate the collision kernel as

$$\mathcal{C}_{2\to 3} = \mathcal{C}^a_{2\to 3} + \mathcal{C}^b_{2\to 3} = \mathcal{C}^>_{2\to 3} + \mathcal{C}^<_{2\to 3}, \tag{43}$$

with

$$\begin{aligned} \mathcal{C}^>_{2\to 3} &= \frac{1}{N_g}\int\frac{d^4q}{(2\pi)^4}\int_{123l}\int_k^{q>k}\frac{2E_l}{2E_p}\int\frac{dl_0}{2\pi}(2\pi)^8\delta^4(p+q-l)\delta^4(p_1-q-p_2) \\ &\quad \times|M^a_{1p\to 23k}|^2[(2\pi)^4\delta^4(l-k-p_3)(g_pg_1f_2f_3f_k - f_pf_1g_2g_3g_k) \\ &\quad +(2\pi)^4\delta^4(l+k-p_3)(g_pg_1g_kf_2f_3 - f_pf_1f_kg_2g_3)], \\ \mathcal{C}^<_{2\to 3} &= \frac{1}{N_g}\int\frac{d^4q}{(2\pi)^4}\int_{123l}\int_k^{q<k}\frac{2E_l}{2E_p}\int\frac{dl_0}{2\pi}(2\pi)^8\delta^4(p+q-l)\delta^4(p_1-q-p_2) \\ &\quad \times[(2\pi)^4\delta^4(l-k-p_3)|M^a_{1p\to 23k}|^2(g_pg_1f_2f_3f_k - f_pf_1g_2g_3g_k) \\ &\quad +(2\pi)^4\delta^4(l+k-p_3)|M^b_{23\to 1kp}|^2(g_pg_1g_kf_2f_3 - f_pf_1f_kg_2g_3)]. \end{aligned}$$

B.1 Simplifying $\mathcal{C}^{>}_{2\to 3}$

Expand the integrand of $\mathcal{C}^{>}_{2\to 3}$ in terms of k and keep the leading order terms:

$$\begin{aligned}
\mathcal{C}^{>}_{2\to 3} \quad &\approx \quad \frac{1}{N_g}\int\frac{d^4q}{(2\pi)^4}\int_{12l}\int_k^{q>k}\frac{1}{2E_p}\int\frac{dl_0}{2\pi}(2\pi)^8\delta^4(p+q-l)\delta^4(p_1-q-p_2)\\
&\quad\times|M^a_{1p\to 23k}|^2[(2\pi)\delta(l_0-|\mathbf{k}|-|\mathbf{l}-\mathbf{k}|)(g_pg_1f_2f_lf_k-f_pf_1g_2g_lg_k)\\
&\quad+(2\pi)\delta(l_0+|\mathbf{k}|-|\mathbf{l}+\mathbf{k}|)(g_pg_1g_kf_2f_l-f_pf_1f_kg_2g_l)]\\
&\approx \quad \frac{1}{N_g}\int\frac{d^4q}{(2\pi)^4}\int_{12l}\int_k^{q>k}\frac{1}{2E_p}\int\frac{dl_0}{2\pi}(2\pi)^8\delta^4(p+q-l)\delta^4(p_1-q-p_2)\\
&\quad\times|M^a_{1p\to 23k}|^2[(2\pi)\delta(l_0-|\mathbf{l}|)(g_pg_1f_2f_lf_k-f_pf_1g_2g_lg_k)\\
&\quad+(2\pi)\delta(l_0-|\mathbf{l}|)(g_pg_1g_kf_2f_l-f_pf_1f_kg_2g_l)]\\
&= \quad \frac{1}{N_g}\int\frac{d^4q}{(2\pi)^4}\int_{12l}\int_k^{q>k}\frac{1}{2E_p}(2\pi)^4\delta^4(p+q-l)(2\pi)^4\delta^4(p_1-q-p_2)\\
&\quad\times|M_{1p\to 2l}|^2\frac{2g^2N_c(p\cdot p_1)}{(p\cdot k)(p_1\cdot k)}(1+2f_k)(g_pg_1f_2f_l-f_pf_1g_2g_l),
\end{aligned}\tag{44}$$

where in the last equality $l^\mu=(|\mathbf{l}|,\mathbf{l})$ is on-shell, and the $2\to 2$ amplitude is

$$|M_{1p\to 2l}|^2 \quad = \quad 32g^4N_c^2N_g\frac{(p\cdot p_1)^2}{(q^2)^2}. \tag{45}$$

We have written the $2\to 3$ amplitude in a form of a $2\to 2$ amplitude times a $1\to 2$ splitting function. Indeed, if for example k is nearly collinear to p,

$$\begin{aligned}
\frac{2g^2N_c(p\cdot p_1)}{(p\cdot k)(p_1\cdot k)} \quad &\approx \quad \frac{2g^2N_c|\mathbf{p}|}{(p\cdot k)|\mathbf{k}|}\\
&= \quad \frac{2g^2}{(p+k)^2}P_{gg}(z)
\end{aligned}\tag{46}$$

with $P_{gg}(z)=2C_A/z$ being the standard unregularized $g\to gg$ splitting function at $z\to 0$ limit where $z=E_k/E_p$ [43, 44, 45].

In the collinear approximation, if $\mathbf{v_k}\simeq\mathbf{v}_1$, then $p\cdot p_1/k\cdot p\approx|\mathbf{p}_1|/|\mathbf{k}|$; or if $\mathbf{v_k}\simeq\mathbf{v}_p$, then $p\cdot p_1/k\cdot p_1\approx|\mathbf{p}|/|\mathbf{k}|$. We have

$$\begin{aligned}
\mathcal{C}^{>}_{2\to 3} \quad &\approx \quad \frac{1}{N_g}\int_{12l}\frac{1}{2E_p}|M_{1p\to 2l}|^2\int_{k<p_1-p_2}\frac{2g^2N_c}{|\mathbf{k}|^2}\left[\frac{1+2f_k}{1-\mathbf{v}_k\cdot\mathbf{v}_1}+\frac{1+2f_k}{1-\mathbf{v}_k\cdot\mathbf{v}_p}\right]\\
&\quad\times(2\pi)^4\delta^4(p+p_1-p_2-l)(g_pg_1f_2f_l-f_pf_1g_2g_l).
\end{aligned}\tag{47}$$

This is essentially a $p+p_1\to p_2+l$ collision kernel with an inner $1\to 2$ splitting function. Let

$$\mathcal{D}(q) \quad = \quad \int_{k<q}\frac{2g^2N_c}{|\mathbf{k}|^2}\left[\frac{1+2f_k}{1-\mathbf{v}_k\cdot\mathbf{v}_1}+\frac{1+2f_k}{1-\mathbf{v}_k\cdot\mathbf{v}_p}\right]. \tag{48}$$

For isotropic distribution,

$$\begin{aligned}
\mathcal{D}(q) &= 2\int_{k<q} \frac{d^3\mathbf{k}}{(2\pi)^3 2E_k} \frac{2g^2 N_c(1+2f_k)}{|\mathbf{k}|^2(1-\cos\theta)} \\
&= 2\frac{g^2 N_c}{(2\pi)^2} \int_0^{|\mathbf{q}|} d|\mathbf{k}| \frac{1+2f_k}{|\mathbf{k}|} \int_0^{\pi} d\theta \frac{\sin\theta}{1-\cos\theta} \\
&= 2\frac{g^2 N_c}{(2\pi)^2} \int_0^{|\mathbf{q}|} d|\mathbf{k}| \frac{1+2f_k}{|\mathbf{k}|} \int_{-1}^{1} \frac{dx}{1-x}. \qquad (49)
\end{aligned}$$

Thus,

$$\begin{aligned}
\mathcal{C}^{>}_{2\to3} \approx{}& \frac{1}{N_g}\int_{12l} \frac{1}{2E_p} |M_{1p\to2l}|^2 \mathcal{D}(p_1-p_2)(2\pi)^4\delta^4(p+p_1-p_2-l) \\
&\times(g_p g_1 f_2 f_l - f_p f_1 g_2 g_l). \qquad (50)
\end{aligned}$$

There are two types of infrared divergence in $\mathcal{D}(q)$. (1) The logarithmic divergence $\int_{-1}^{1} dx/(1-x) \sim \int d\theta/\theta \sim \ln(1/\theta_m)$ with θ_m the minimal angle between $\mathbf{k}$ and $\mathbf{p}$. θ_m arises completely due to interaction, so $\theta_m \sim g$. Thus, $\int_{-1}^{1} dx/(1-x) \sim \ln(1/g)$ in both glasma and nearly thermal equilibrium. (2) Near thermal equilibrium, $f_k \sim T/\omega_k$, thus $\int_0^q (dk/k)(1+2f_k) \sim 2T\int_0^q (dkk/(k^2+m_\infty^2)^{3/2} \sim T(1/m_\infty - 1/m_D)$ where we use m_∞ to denote the mass of the emitted or absorbed ultrasoft gluon k and m_D to denote the mass of the exchanged gluon q. Near equilibrium, both m_∞ and m_D are of order gT but can have different prefactors, we find $\mathcal{D}(q) \sim g\ln(1/g)$. In the initial glasma, $m_D \sim m_\infty \sim Q_s$ and $f_k \sim 1/\alpha_s$, thus $\int_0^q (dk/k)(1+2f_k) \sim (2/\alpha_s)\ln(q/m_\infty) \sim 1/\alpha_s$. Thus $\mathcal{D}(q) \sim \ln(1/g)$. As the glasma evolves, $f_k \sim \Lambda_S/(\alpha_s k)$, if $m_D \sim m_\infty \sim \sqrt{\Lambda\Lambda_S}$, thus $\int_0^q (dk/k)(1+2f_k) \sim (1/\alpha_s)(\Lambda_S/m_\infty) \sim (1/\alpha_s)\sqrt{\Lambda_S/\Lambda}$. Thus, we find $\mathcal{D}(q) \sim \sqrt{\Lambda_S/\Lambda}\ln(1/g)$.

In any case, we can conclude that the ratio of ultrasoft gluon emission and absorbtion $2\to3$ processes over the elastic $2\to2$ processes is either $\ln(1/g)$ order or $g\ln(1/g)$ order.

B.2 Simplifying $\mathcal{C}^{<}_{2\to3}$

Expand the distribution functions in $\mathcal{C}^{<}_{2\to3}$ in terms of q and keep the leading order terms:

$$\begin{aligned}
\mathcal{C}^{<}_{2\to3} \approx{}& \frac{1}{N_g}\int \frac{d^4q}{(2\pi)^4} \int_{123} \int_k^{q<k} \frac{1}{2E_p} (2\pi)^4\delta^4(p_1-q-p_2)h_1 \\
&\times[(2\pi)^4\delta^4(p+q-k-p_3)|M^a_{1p\to23k}|^2(g_p f_3 f_k - f_p g_3 g_k) \\
&+(2\pi)^4\delta^4(p+q+k-p_3)|M^b_{23\to1kp}|^2(g_p g_k f_3 - f_p f_k g_3)] \\
\approx{}& \frac{1}{N_g}\int \frac{d^4q}{(2\pi)^4} \int_{13} \int_k^{q<k} \frac{1}{2E_p 2E_1} (2\pi)\delta(q_0-\mathbf{q}\cdot\mathbf{v}_1)|M^a_{1p\to23k}|^2 h_1 \\
&\times[(2\pi)^4\delta^4(p+q-k-p_3)|M^a_{1p\to23k}|^2(g_p f_3 f_k - f_p g_3 g_k) \\
&+(2\pi)^4\delta^4(p+q+k-p_3)|M^b_{23\to1kp}|^2(g_p g_k f_3 - f_p f_k g_3)],
\end{aligned}$$

where $h_1 \equiv f_1 g_1$. This is basically a $1 \to 2$ collision kernel with the $2 \to 2$ processes playing a role of opening a finite phase space for $1 \to 2$ process. Because q is small, p, k and p_3 are nearly collinear (there is no phase space at the collinear region $k \parallel p_1$). In the collinear approximation, we have

$$\begin{aligned} p_0 + q_0 - k_0 - p_{30} &\approx q_0 - |\mathbf{k}| - (\mathbf{q} - \mathbf{k}) \cdot \mathbf{v}_p \approx q_0 - \mathbf{q} \cdot \mathbf{v}_p, \\ p_0 + q_0 + k_0 - p_{30} &\approx q_0 + |\mathbf{k}| - (\mathbf{q} + \mathbf{k}) \cdot \mathbf{v}_p \approx q_0 - \mathbf{q} \cdot \mathbf{v}_p. \end{aligned}$$

The amplitudes are

$$|M^a_{1p\to 23k}|^2 = 64 g^6 N_c^3 N_g \frac{(p \cdot p_1)^2}{(q^2)^2 |\mathbf{k}|^2 (1 - \mathbf{v}_p \cdot \mathbf{v}_k)}, \tag{51}$$

$$|M^b_{23\to 1kp}|^2 = 64 g^6 N_c^3 N_g \frac{|\mathbf{p}| + |\mathbf{k}|}{|\mathbf{k}|} \frac{(p \cdot p_1)^2}{(q^2)^2 |\mathbf{k}|^2 (1 - \mathbf{v}_p \cdot \mathbf{v}_k)}. \tag{52}$$

Thus,

$$\begin{aligned} \mathcal{C}^<_{2\to 3} \approx\ & \frac{1}{N_g} \int \frac{d^4 q}{(2\pi)^4} \int_1 \int_k^{q<k} \frac{1}{(2E_p)^2 2E_1} (2\pi)\delta(q_0 - \mathbf{q} \cdot \mathbf{v}_1)(2\pi)\delta(q_0 - \mathbf{q} \cdot \mathbf{v}_p) h_1 \\ \times\ & \left[|M^a_{1p\to 23k}|^2 (g_p f_{p-k} f_k - f_p g_{p-k} g_k) + |M^b_{23\to 1kp}|^2 (g_p g_k f_{p+k} - f_p f_k g_{p+k}) \right]. \end{aligned} \tag{53}$$

In the following we denote $q = |\mathbf{q}|, p = |\mathbf{p}|, p_1 = |\mathbf{p}_1|, k = |\mathbf{k}|$. Let $q_0 = xq$ and let $\mathbf{v}_p = (1, 0, 0)$, $\mathbf{v}_1 = (\cos\theta_1, \sin\theta_1, 0)$, and $\mathbf{v}_q = (\sin\theta_q \cos\phi_q, \sin\theta_q \sin\phi_q, \cos\theta_q)$.

$$\begin{aligned} & \delta(x - \mathbf{v}_q \cdot \mathbf{v}_1)\delta(x - \mathbf{v}_q \cdot \mathbf{v}_p) = \delta[x - \sin\theta_q \cos(\theta_1 - \phi_q)]\delta(x - \sin\theta_q \cos\phi_q) \\ =\ & \frac{1}{\sin\theta_q} \frac{\delta(x - \sin\theta_q \cos\phi_q)}{|\sin\phi_q - \sin(\phi_q - \theta_1)|} \left[\delta\left(\phi_q - \frac{\theta_1}{2}\right) + \delta\left(\phi_q - \frac{\theta_1}{2} - \pi\right) \right] \\ =\ & \frac{1}{\sin\theta_q} \frac{1}{2\sin(\theta_1/2)} \left[\delta\left(\phi_q - \frac{\theta_1}{2}\right) \delta\left(x - \sin\theta_q \cos\frac{\theta_1}{2}\right) \right. \\ & \left. + \delta\left(\phi_q - \frac{\theta_1}{2} - \pi\right) \delta\left(x + \sin\theta_q \cos\frac{\theta_1}{2}\right) \right]. \end{aligned}$$

Thus,

$$\begin{aligned} & \int \frac{dq_0}{2\pi} d\Omega_q (2\pi)\delta(q_0 - \mathbf{q} \cdot \mathbf{v}_1)(2\pi)\delta(q_0 - \mathbf{q} \cdot \mathbf{v}_p) |M^a_{1p\to 23k}|^2 \\ =\ & 128\pi g^6 N_c^3 N_g \frac{(pp_1)^2}{q^5 k^2} \int dx \int_0^\pi d\theta_q \sin\theta_q \int_0^{2\pi} d\phi_q \delta(x - \mathbf{v}_q \cdot \mathbf{v}_1)\delta(x - \mathbf{v}_q \cdot \mathbf{v}_p) \\ & \times \frac{(1 - \mathbf{v}_p \cdot \mathbf{v}_1)^2}{(1 - x^2)^2 (1 - \mathbf{v}_p \cdot \mathbf{v}_k)} \\ =\ & 128\pi g^6 N_c^3 N_g \frac{(pp_1)^2}{q^5 k^2} \frac{(1 - \mathbf{v}_p \cdot \mathbf{v}_1)^2}{1 - \mathbf{v}_p \cdot \mathbf{v}_k} \int_0^\pi d\theta_q \frac{1}{\sin\frac{\theta_1}{2} (1 - \sin^2\theta_q \cos^2\frac{\theta_1}{2})^2} \\ =\ & 128\pi^2 g^6 N_c^3 N_g \frac{(pp_1)^2}{q^5 k^2} \frac{3 - \mathbf{v}_p \cdot \mathbf{v}_1}{1 - \mathbf{v}_p \cdot \mathbf{v}_k}. \end{aligned} \tag{54}$$

Furthermore, for isotropic distributions, we have:

$$
\begin{aligned}
\mathcal{C}^{<}_{2\to 3} &= \frac{128\pi^2 g^6 N_c^3 N_g}{N_g} \int_0^\infty \frac{dq q^2}{(2\pi)^3} \int_1 \int_k^{q<k} \frac{1}{(2E_p)^2 2E_1} \frac{(pp_1)^2}{q^5 k^2} \frac{3 - \mathbf{v}_p \cdot \mathbf{v}_1}{1 - \mathbf{v}_p \cdot \mathbf{v}_k} h_1 \\
&\quad \times \left[(g_p f_{p-k} f_k - f_p g_{p-k} g_k) + \frac{(p+k)^3}{p^3} (g_p g_k f_{p+k} - f_p f_k g_{p+k}) \right] \\
&= \frac{3 g^6 N_c^3}{16\pi^5} \int_0^\infty dp_1 p_1^2 h_1 \int_{-1}^{1} \frac{dx}{1-x} \int_0^\infty \frac{dq}{q^3} \int_q^\infty \frac{dk}{k} \\
&\quad \times \left[(g_p f_{p-k} f_k - f_p g_{p-k} g_k) + \frac{(p+k)^3}{p^3} (g_p g_k f_{p+k} - f_p f_k g_{p+k}) \right], \quad (55)
\end{aligned}
$$

where the upper limit of the integration over k for the first two terms should be cut at p. When k is small the integrand over k goes like $(1+2f_p)f'_p$. It is finite, so we can put the lower limit of $\int dk$ as 0. In the first two terms, let $k = zp$ with z being the momentum fraction of the emitted gluon; in the last two terms let $k = z(p+k)$ with z being the momentum fraction of the absorbed gluon. Then we have

$$
\begin{aligned}
\mathcal{C}^{<}_{2\to 3} &= \xi \alpha_s^2 R \frac{I_a}{I_b} \int_0^{z_c} \frac{dz}{z} \Big\{ \left[g_p f_{(1-z)p} f_{zp} - f_p g_{(1-z)p} g_{zp} \right] \\
&\quad + \frac{1}{(1-z)^4} \left[g_p g_{zp/(1-z)} f_{p/(1-z)} - f_p f_{zp/(1-z)} g_{p/(1-z)}) \right] \Big\}, \quad (56)
\end{aligned}
$$

where we introduce the momentum fraction cut $z_c < 1$ to characterizing that k being a small fraction of the total momentum in this effective $1 \to 2$ process and the prefactor R is given by

$$
R \equiv \frac{12 N_c^3}{\pi^2} \frac{1}{\xi} \int_{-1}^{1} \frac{dx}{1-x} m_D^2 \int_0^\infty \frac{dq}{q^3} \sim \hat{O}(1). \quad (57)
$$

There are two kinds of infrared divergences in $\mathcal{C}^{<}_{2\to 3}$: (1) The logarithmic divergence: $\int_{-1}^{1} dx/(1-x) \sim \ln(1/g)$. (2) The quadratic divergence $\int dq/q^3 \sim 1/m_D^2$. Noticing that $\mathcal{C}_{2\to 2}$ is of order $\alpha_s^2 \ln(1/g)$ near equilibrium and $(Q_s/\alpha_s)\ln(1/g)$ in initial glasma state, we find that $\mathcal{C}^{<}_{2\to 3}/\mathcal{C}_{2\to 2}$ is of order $\hat{O}(1)$ in both equilibrium and initial glasma states.

Now we show that the collision kernel $\mathcal{C}^{<}_{2\to 3}$ conserves energy, i.e, $\int_0^\infty dp p^3 \mathcal{C}^{<}_{2\to 3}[f_p] = 0$:

$$
\begin{aligned}
\int_0^\infty dp p^3 \mathcal{C}^{<}_{2\to 3}[f_p] &\propto \int_0^\infty dp p^3 \int_0^{z_c} \frac{dz}{z} \Big\{ \left[g_p f_{(1-z)p} f_{zp} - f_p g_{(1-z)p} g_{zp} \right] \\
&\quad + \frac{1}{(1-z)^4} \left[g_p g_{zp/(1-z)} f_{p/(1-z)} - f_p f_{zp/(1-z)} g_{p/(1-z)}) \right] \Big\}.
\end{aligned}
$$

In the last two terms, change the variable $p \to (1-z)p$, one finds that the first two terms cancel the last two terms so that $\int_0^\infty dp p^3 \mathcal{C}^{<}_{2\to 3}[f_p] = 0$.

References

[1] L. D. McLerran and R. Venugopalan, Phys. Rev. D **49**, 2233 (1994) [hep-ph/9309289]. L. D. McLerran and R. Venugopalan, Phys. Rev. D **49**, 3352 (1994) [hep-ph/9311205].

[2] J. P. Blaizot and A. H. Mueller, Nucl. Phys. **B289**, 847 (1987).

[3] E. Iancu and R. Venugopalan, In *Hwa, R.C. (ed.) et al.: Quark gluon plasma* 249-3363. [hep-ph/0303204]; H. Weigert, Prog. Part. Nucl. Phys. **55**, 461-565 (2005). [hep-ph/0501087]; F. Gelis, E. Iancu, J. Jalilian-Marian and R. Venugopalan, Ann. Rev. Nucl. Part. Sci. **60**, 463-489 (2010). [arXiv:1002.0333 [hep-ph]].

[4] P. Romatschke and R. Venugopalan, Phys. Rev. Lett. **96**, 062302 (2006) [arXiv:hep-ph/0510121]; P. Romatschke and R. Venugopalan, Phys. Rev. D **74**, 045011 (2006) [arXiv:hep-ph/0605045]; P. Romatschke and R. Venugopalan, Eur. Phys. J. **A29**, 71-75 (2006). [hep-ph/0510292].

[5] T. Lappi and L. McLerran, Nucl. Phys. **A772**, 200-212 (2006). [hep-ph/0602189].

[6] U. W. Heinz, in 'Relativistic Heavy Ion Physics', Landolt-Boernstein New Series, I/23, edited by R. Stock (Springer Verlag, New York,2010) Chap. 5 [arXiv:0901.4355 [nucl-th]]. U. W. Heinz and R. Snellings, arXiv:1301.2826 [nucl-th].

[7] A. H. Mueller, Nucl. Phys. B **572**, 227 (2000) [arXiv:hep-ph/9906322]; Phys. Lett. B **475**, 220 (2000) [arXiv:hep-ph/9909388].

[8] R. Baier, A. H. Mueller, D. Schiff, and D. T. Son, Phys. Lett. B **502**, 51 (2001) [arXiv:hep-ph/0009237]; R. Baier, A. H. Mueller, D. T. Son, and D. Schiff, Nucl. Phys. A **698**, 217 (2002).

[9] A. H. Mueller, A. I. Shoshi, and S. M. H. Wong, Phys. Lett. **B632**, 257-260 (2006). [hep-ph/0505164]; A. H. Mueller, A. I. Shoshi, and S. M. H. Wong, Eur. Phys. J. **A29**, 49-52 (2006). [hep-ph/0512045]. A. H. Mueller, A. I. Shoshi, and S. M. H. Wong, Nucl. Phys. **B760**, 145-165 (2007). [hep-ph/0607136].

[10] P. B. Arnold, J. Lenaghan, and G. D. Moore, JHEP **0308**, 002 (2003). [hep-ph/0307325].

[11] S. Mrowczynski, Phys. Lett. **B314**, 118-121 (1993); S. Mrowczynski, Acta Phys. Polon. **B37**, 427-454 (2006).

[12] P. Romatschke and M. Strickland, Phys. Rev. **D68**, 036004 (2003). [hep-ph/0304092]; P. Romatschke and M. Strickland, Phys. Rev. **D69**, 065005 (2004). [hep-ph/0309093].

[13] A. Rebhan, P. Romatschke, and M. Strickland, JHEP **0509**, 041 (2005) [arXiv:hep-ph/0505261].

[14] Z. Xu and C. Greiner, Phys. Rev. C **71**, 064901 (2005) [hep-ph/0406278].

[15] J. -P. Blaizot, F. Gelis, J. -F. Liao, L. McLerran, and R. Venugopalan, Nucl. Phys. A **873**, 68 (2012). [arXiv:1107.5296 [hep-ph]].

[16] J. -P. Blaizot, J. Liao, and L. McLerran, in final preparation.

[17] A. Kurkela and G. D. Moore, JHEP **1112**, 044 (2011) [arXiv:1107.5050 [hep-ph]].

[18] A. Kurkela and G. D. Moore, JHEP **1111**, 120 (2011) [arXiv:1108.4684 [hep-ph]].

[19] T. Epelbaum and F. Gelis, Nucl. Phys. A **872**, 210 (2011) [arXiv:1107.0668 [hep-ph]].

[20] F. Gelis, arXiv:1110.1544 [hep-ph].

[21] J. Berges and D. Sexty, Phys. Rev. Lett. **108**, 161601 (2012) [arXiv:1201.0687 [hep-ph]].

[22] J. Berges, S. Scheffler, S. Schlichting, and D. Sexty, Phys. Rev. D **85**, 034507 (2012) [arXiv:1111.2751 [hep-ph]].

[23] J. Berges, S. Schlichting, and D. Sexty, arXiv:1203.4646 [hep-ph].

[24] J. Berges and S. Schlichting, arXiv:1209.0817 [hep-ph].

[25] A. Kurkela and G. D. Moore, arXiv:1207.1663 [hep-ph].

[26] S. Schlichting, arXiv:1207.1450 [hep-ph].

[27] J. Berges, J. -P. Blaizot, and F. Gelis, J. Phys. G G **39**, 085115 (2012) [arXiv:1203.2042 [hep-ph]].

[28] J. Berges, K. Boguslavski, S. Schlichting, and R. Venugopalan, arXiv:1303.5650 [hep-ph].

[29] M. Attems, A. Rebhan, and M. Strickland, Phys. Rev. D **87**, 025010 (2013) [arXiv:1207.5795 [hep-ph]].

[30] M. Chiu, T. K. Hemmick, V. Khachatryan, A. Leonidov, J. Liao, and L. McLerran, arXiv:1202.3679 [nucl-th].

[31] J. -P. Blaizot, F. Gelis, J. Liao, L. McLerran, and R. Venugopalan, arXiv:1210.6838 [hep-ph].

[32] J. Liao, arXiv:1209.2998 [hep-ph].

[33] E. Braaten and R. D. Pisarski, Nucl. Phys. **B337**, 569 (1990).

[34] J. -P. Blaizot and E. Iancu, Phys. Rept. **359**, 355 (2002) [hep-ph/0101103].

[35] J. Liao and E. Shuryak, Phys. Rev. C **75**, 054907 (2007); Phys. Rev. Lett. **101**, 162302 (2008); Phys. Rev. Lett. **102**, 202302 (2009); Phys. Rev. Lett. **109**, 152001 (2012).

[36] J. F. Gunion and G. Bertsch, Phys. Rev. D **25**, 746 (1982).

[37] P. B. Arnold, G. D. Moore, and L. G. Yaffe, JHEP **0011**, 001 (2000) [hep-ph/0010177]. P. B. Arnold, G. D. Moore, and L. G. Yaffe, JHEP **0305**, 051 (2003) [hep-ph/0302165]. P. B. Arnold, C. Dogan, and G. D. Moore, Phys. Rev. D **74**, 085021 (2006) [hep-ph/0608012].

[38] Z. Xu, C. Greiner, and H. Stocker, Phys. Rev. Lett. **101**, 082302 (2008) [arXiv:0711.0961 [nucl-th]]. O. Fochler, J. Uphoff, Z. Xu, and C. Greiner, arXiv:1302.5250 [hep-ph]. A. El, F. Lauciello, C. Wesp, Z. Xu, and C. Greiner, arXiv:1207.5331 [hep-th].

[39] J. -W. Chen, H. Dong, K. Ohnishi, and Q. Wang, Phys. Lett. B **685**, 277 (2010) [arXiv:0907.2486 [nucl-th]]. J. -W. Chen, J. Deng, H. Dong, and Q. Wang, Phys. Rev. C **87**, 024910 (2013) [arXiv:1107.0522 [hep-ph]]. J. -W. Chen, Y. -F. Liu, Y. -K. Song, and Q. Wang, arXiv:1212.5308 [hep-ph].

[40] F. A. Berends, R. Kleiss, P. De Causmaecker, R. Gastmans, and T. T. Wu, Phys. Lett. B **103**, 124 (1981).

[41] R. Abir, C. Greiner, M. Martinez, and M. G. Mustafa, Phys. Rev. D **83**, 011501 (2011) [arXiv:1011.4638 [nucl-th]].

[42] T. Bhattacharyya, S. Mazumder, S. KDas, and J. -eAlam, Phys. Rev. D **85**, 034033 (2012) [arXiv:1106.0609 [nucl-th]].

[43] G. Altarelli and G. Parisi, Nucl. Phys. B **126**, 298 (1977).

[44] V. N. Gribov and L. N. Lipatov, Sov. J. Nucl. Phys. **15**, 438 (1972) [Yad. Fiz. **15**, 781 (1972)].

[45] Y. L. Dokshitzer, Sov. Phys. JETP **46**, 641 (1977) [Zh. Eksp. Teor. Fiz. **73**, 1216 (1977)].